Articles

Block Copolymer Micelles as Nanocontainers for Controlled Release of Proteins from Biocompatible Oil Phases

Andrew C. Miller,[†] Anna Bershteyn,[‡] Wuisiew Tan,[‡] Paula T. Hammond,[†,§]
Robert E. Cohen,[†] and Darrell J. Irvine[*,‡,§,‖]

Department of Chemical Engineering, Department of Materials Science and Engineering, Koch Institute for Integrative Cancer Research, and Department of Biological Engineering, Massachusetts Institute of Technology, 77 Massachusetts Avenue, Cambridge, Massachusetts 02139

Biocompatible oils are used in a variety of medical applications ranging from vaccine adjuvants to vehicles for oral drug delivery. To enable such nonpolar organic phases to serve as reservoirs for delivery of hydrophilic compounds, we explored the ability of block copolymer micelles in organic solvents to sequester proteins for sustained release across an oil−water interface. Self-assembly of the block copolymer, poly(ϵ-caprolactone)-*block*-poly(2-vinyl pyridine) (PCL-*b*-P2VP), was investigated in toluene and oleic acid, a biocompatible naturally occurring fatty acid. Micelle formation in toluene was characterized by dynamic light scattering (DLS) and atomic force microscopy (AFM) imaging of micelles cast onto silicon substrates. Cryogenic transmission electron microscopy confirmed a spherical morphology in oleic acid. Studies of homopolymer solubility implied that micelles in oleic acid consist of a P2VP corona and a PCL core, while P2VP formed the core of micelles assembled in toluene. The loading of two model proteins (ovalbumin (ova) and bovine serum albumin (BSA)) into micelles was demonstrated with loadings as high as 7.8% wt of protein per wt of P2VP in oleic acid. Characterization of block copolymer morphology in the two solvents after protein loading revealed spherical particles with similar size distributions to the as-assembled micelles. Release of ova from micelles in oleic acid was sustained for 12−30 h upon placing the oil phase in contact with an aqueous bath. Unique to the situation of micelle assembly in an oily phase, the data suggest protein is sequestered in the P2VP *corona* block of PCL-*b*-P2VP micelles in oleic acid. More conventionally, protein loading occurs in the P2VP *core* of micelles assembled in toluene.

Introduction

Selective solvents induce the self-assembly of block copolymers in solution into stable ordered structures. In medical applications, amphiphilic block copolymer micelles assembled in aqueous solutions with a hydrophilic corona block and hydrophobic core block have long been of interest as carriers for drug delivery.[1−7] A variety of aqueous micelle systems that sequester poorly water-soluble drugs in the micelle core[1−7] or which carry compounds that interact specifically with the core block (e.g., oligonucleotides bound to ionic micelles[8]) have been developed for systemic drug delivery and cancer therapy.

In a similar manner, micellar systems assembled in nonpolar solvents have been used as carriers of hydrophilic compounds. Metal salts sequestered into the hydrophilic cores of block copolymer micelles in organic solutions and cast as micellar thin films have been of particular interest for a variety of applications.[9−32] Micelles have also been used as carriers of polar small molecule dyes in organic solutions. For example, Il Yoo et al.[33] loaded rhodamine derivatives in PS-*b*-P4VP inverse micelles in toluene and Groβ and Maskos[34] used cross-linked PS-*b*-P2VP nanoparticles in toluene to encapsulate low molec-ular weight dyes. Star polymer architectures and polyorganosiloxane nanoparticles have also been used for solubilizing low molecular weight dyes in organic phases.[35−37]

While most of these prior studies have focused on solvents relevant for industrial applications, we hypothesized that block copolymer micelles formed in biocompatible oil phases could be of interest in biomedical applications as carriers for therapeutic molecules, imaging agents, or vaccine adjuvants. Biocompatible oils are found in a variety of medical applications: Important vaccine adjuvants used widely in animal research (e.g., Freund's adjuvant) and in human patients (e.g., MF-59, a vaccine adjuvant in clinical use in the European Union) are based on oils (mineral oil and squalene in the case of Freund's adjuvant and MF-59,[38,39] respectively). Because of their interaction with lipid membranes, oils have been investigated for drug delivery applications such as transdermal[40−42] and oral delivery.[43] Other well-studied oils for biomedical applications include lipiodol, an iodinated fatty acid ethyl ester, used as a imaging contrast agent[44] to target radiotherapy to hepatocellular carcinoma[45] and even for infertility.[46]

Although micelles formed by block or branched copolymers could be useful for controlling the loading and release of proteins or other hydrophilic drugs from oil phases relevant to many of the biomedical applications highlighted above, very few studies of micellar systems in biocompatible oil phases for drug delivery have been reported. In the arena of biotechnology, protein

* To whom correspondence should be addressed. E-mail: djirvine@mit.edu.
† Department of Chemical Engineering.
‡ Department of Materials Science and Engineering.
§ Koch Institute for Integrative Cancer Research.
‖ Department of Biological Engineering.

loading into surfactant-based inverse micelles has been used as a strategy for extraction/purification of proteins in a variety of organic solvents,[47−56] including fatty acids and fatty acid esters.[55,56] New and Kirby[57] investigated low molecular weight amphiphiles for loading of calcintonin in biocompatible oil phases for oral delivery. Recent work by Jones et al.[58] demonstrated the loading of a peptide, vasopressin, and two proteins, myoglobin and bovine serum albumin, into lipid-modified poly(glycerol methacrylate) star polymers in ethyl oleate.

In this work we focused on micelles formed from a block copolymer system poly(ε-caprolactone)-*block*-poly(2-vinyl pyridine) (PCL-*b*-P2VP), containing a biodegradable hydrophobic block (PCL) and a polar, hydrogen bonding block (P2VP). We examined micelle assembly in two different oil phases, toluene (as a model volatile nonpolar solvent), and oleic acid, a naturally occurring fatty acid. Oleic acid is a biocompatible oil used in oral drug delivery,[43,59−63] buccal delivery,[64] transdermal drug delivery,[40−42,65] and as a vaccine adjuvant.[66] PCL-*b*-P2VP micelles in toluene were characterized by atomic force microscopy (AFM) and dynamic light scattering. The structure of the block copolymer in oleic acid was studied via cryogenic transmission electron microscopy (cryoTEM). Notably, we observed different micellar structures in the two solvents used here. In toluene, the micelles consist of P2VP cores with PCL corona, while in oleic acid our results suggest PCL blocks compose the micelle core with P2VP forming the corona. Two proteins, ovalbumin (ova) and bovine serum albumin (BSA), were loaded into the organic phase micelles. When the protein-loaded oleic acid phase is placed in contact with an aqueous reservoir, sustained release of protein back into aqueous solution is maintained over a period of ∼30 h. These results highlight the potential of block copolymers as carriers for sustained release of hydrophilic drug cargos from biocompatible oils.

Experimental Section

Materials. Poly(ε-caprolactone)-*block*-poly(2-vinyl pyridine) (PCL-*b*-P2VP) diblock copolymer [M_n (PCL) = 35400 g/mol, M_n (P2VP) = 20900 g/mol, copolymer PDI (M_w/M_n) = 1.8], PCL homopolymer [M_n = 33000 g/mol, PDI = 1.7], P2VP homopolymer [M_n = 22000 g/mol, PDI = 1.09] and their molecular characterization data were purchased from Polymer Source, Inc. Toluene and gold(III) chloride trihydrate were obtained from Sigma-Aldrich. Phosphate buffered saline (PBS) was purchased from VWR International. Ovalbumin, texas red (ova-TR) conjugate, bovine serum albumin, texas red (BSA-TR) conjugate, NuPAGE LDS sample buffer, MES SDS running buffer, BenchMark prestained protein ladder, and 10% Bis-Tris gels were obtained from Invitrogen. All aqueous solutions were made using deionized (DI) water (>18 MΩ cm, Millipore Milli-Q). Oleic acid was obtained from EMD Chemicals and [methyl-C[14]] methylated ovalbumin (ova-C[14]) was purchased from American Radiolabeled Chemicals, Inc. Hionic-Fluor scintillation cocktail was obtained from Perkin-Elmer. All chemicals were used as received. Quantifoil R1.2/1.3 holey carbon-coated copper TEM grids were obtained from Ted Pella, Inc. Silicon nitride window TEM grids were obtained from Structure Probe, Inc.

Preparation of Polymer Solutions. Toluene or oleic acid was added to polymer powder to form a 10 g/L polymer solution. The solution was heated in a sealed vial at 70 °C for 2 h with periodic agitation to fully dissolve the polymer. Polymer solutions were then allowed to cool to room temperature for 16 h. Toluene copolymer solutions were centrifuged for 30 s at 14000*g* before use. No precipitates or sediments were observed in these solutions. Dilutions as needed were made from these stock solutions.

Atomic Force Microscopy (AFM). Imaging was performed on a Digital Instruments Dimension 3000 Nanoscope IIIA scanning probe

microscope using a silicon RTESP cantilever (tip radius <10 nm) from Veeco Instruments operating in tapping mode. Micelle diameter and height were determined using linescan analysis of AFM images with NanoScope Software v5.30. To create samples for imaging, 50 μL of 0.01 g/L polymer solution in toluene were pipetted onto a silicon substrate and spin-cast at 2500 rpm for 60 s with a ramp time of 1 s. Samples were then dried under vacuum for at least 12 h at 25 °C prior to imaging. For cavitation, micelle-coated substrates were placed in 20 mL of PBS for 16 h, rinsed briefly with DI water to help remove residual salt from the surface and dried under vacuum for at least 12 h at 25 °C prior to AFM imaging.

Dynamic Light Scattering (DLS). DLS experiments were performed using a Brookhaven BI-200SM light scattering system (514 nm argon laser) at a measurement angle of 90°. Samples (three independent solutions per condition) were measured for 5 min with a polymer concentration of 0.1 g/L in toluene. Number average diameters are reported.

Cryogenic Transmission Electron Microcopy (cryoTEM). CryoTEM was performed to characterize the morphology of micelles in oleic acid. Oleic acid controls without polymer were also examined. A thin film of oleic acid polymer solution was spin cast onto a silicon substrate at 4000 rpm with a 1 s ramp time. A Quantifoil R1.2/1.3 holey carbon-coated copper grid was treated in an oxygen plasma for 30 s and then gently placed into contact with the thin film to transfer oleic acid polymer solution to the TEM grid. The grid was plunged into liquid nitrogen, vitrifying the solution. The grid was then directly loaded into a JEOL 2200FS TEM using a Gatan 626 cryo-specimen holder at liquid nitrogen temperature, and imaged using 200 kV accelerating voltage with a 185 μA emission current. TEM images were recorded at a magnification of 40000× on a slow-scan CCD camera (Gatan, Inc.).

Loading of Metal Salt in PCL-*b*-P2VP Micelles in Toluene. Gold(III) chloride trihydrate solid was added to a 10 mg/mL toluene solution of PCL-*b*-P2VP and mixed on a vortexer at 200 rpm for 16 h. The micelle solution was then decanted from the remaining gold salt and centrifuged for 30 s at 14000*g*. Thin films were then cast onto silicon nitride TEM window grids at 2000 rpm with a 1 s ramp. TEM imaging was performed on a JEOL 200CX operating at 200 keV.

Loading of Proteins in PCL-*b*-P2VP Micelles. To load protein into PCL-*b*-P2VP, 50 μL of 10 g/L protein (ova-TR, BSA-TR, ova-C[14]) was agitated on a vortexer at 200 rpm for 72 h with 1 mL of 10 g/L of polymer solution in oleic acid or toluene in a 1.5 mL microcentrifuge tube at 25 °C. The mixture was then centrifuged to separate the oil and aqueous phases. Oleic acid solutions were centrifuged for 15 min at 14000*g*, while toluene solutions were centrifuged for 30 s at 14000*g*. Ova-C[14] was diluted between 10:1 and 50:1 with nonlabeled ova for loading experiments. Control experiments with no polymer, PCL homopolymer and P2VP homopolymer were also performed. Protein concentrations in each solution were determined using a Molecular Devices Spectramax M2[e] fluorescence plate reader with an excitation and emission wavelength of 584 and 612 nm, respectively. Fluorescence was converted to protein mass/concentration using standard curves prepared from PBS solutions containing 1% BSA and ova-TR in known serial dilutions; this assay was very sensitive and readily detected ova levels down to 10 ng/mL protein. Ova-C[14] concentrations were measured with a Packard Top Count NXT microplate scintillation counter using Hionic-Fluor scintillation cocktail.

Release of Ova-TR into PBS Reservoirs by Static Incubation. Protein release was investigated by gently layering 100 μL of oleic acid or toluene polymer solution loaded with ova-TR (10 mg/mL polymer, 0.29 mg/mL ova-TR) on top of 1 mL of PBS with 1 wt %/v BSA in a 1.5 mL microcentrifuge tube or 5 mL of PBS/BSA in 15 mL polypropylene centrifuge tubes and incubating the quiescent two-phase system at 37 or 25 °C. The oil/aq phase interfacial area during release was ∼0.64 cm² for the 1 mL aq reservoir studies and ∼1.77 cm² for the 5 mL aq reservoir experiments. At various times, aliquots of both phases were taken and their protein concentration determined by
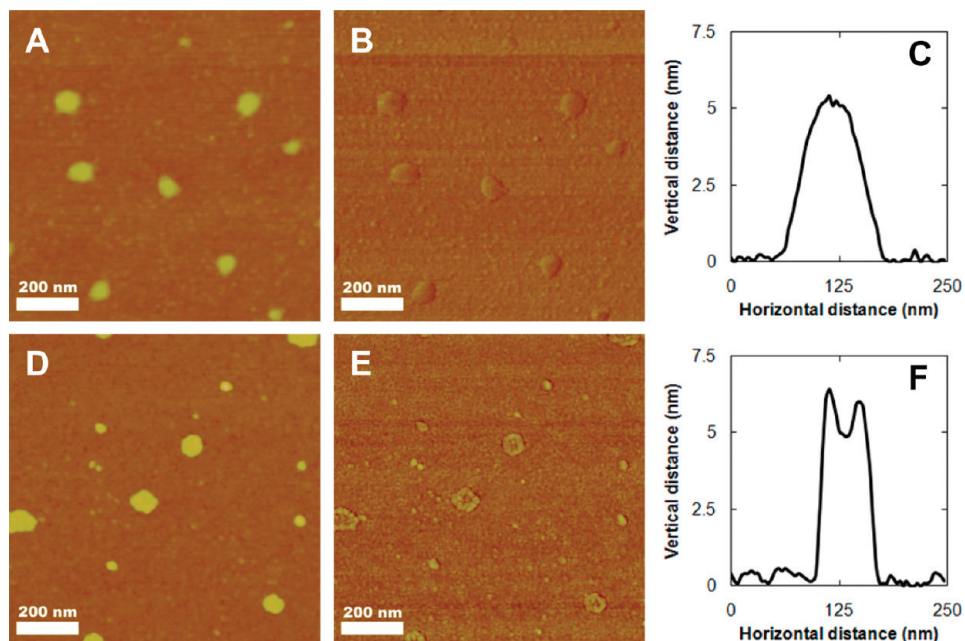
Figure 1. PCL-*b*-P2VP micelles cast from toluene on silicon: (A) AFM height image and (B) corresponding phase image of as-cast micelles; (C) height cross-section of as-cast individual micelle; (D) height image and (E) corresponding phase image of micelles after treatment in PBS for 16 h; and (F) height cross-section showing cavitated morphology of micelles after PBS treatment. Height scales are 20 nm and phase scales are 50°.

fluorescence spectrometry as described above. The oil phase was first removed before an aliquot of the aqueous phase was taken. Individual samples were used only for a single time point and each time point was assayed in quadruplicate. The solutions were not mixed during the release experiment. Samples were kept in the dark throughout the experiments.

SDS PAGE of Ova-TR. Ova-TR was released from oleic acid micelle into a PBS reservoir without BSA. Aliquots were taken after 24 h, and samples were prepared with NuPAGE LDS sample buffer under reducing conditions. Bis-Tris 10% gels with MES SDS running buffer were used at 100 V for 70 min. Staining was performed using a SilverSNAP II stain kit according to the manufacturer's instructions.

Results and Discussion

Characterization of PCL-*b*-P2VP Self-Assembly in Toluene. We first examined micelle formation of PCL-*b*-P2VP in toluene. Toluene is not itself a biocompatible organic phase, but rather serves as a model nonpolar organic phase for analysis of PCL-*b*-P2VP micelle formation and enabled comparison of the properties of this block copolymer with a number of other micelle-forming copolymers that have been extensively characterized in toluene by our group and others. Self-assembly in toluene has been studied for a variety of block copolymers, most notably poly(styrene-*block*-X-vinylpyridine)[28,67,68] (PS-*b*-PXVP; X = 2 or 4) and our own previous work with polystyrene-*block*-poly(acrylic acid)[9,16,69] (PS-*b*-PAA). Toluene is a selective solvent for the PS block and leads to inverse micelle formation for these amphiphilic block copolymers. Block copolymer micellar films can be cast onto substrates from volatile solvents, unlike low molecular weight surfactant micelles, due to the slower exchange kinetics of individual molecules with micelles in solution.[70] The micelle morphology is kinetically trapped in the final thin film upon solvent evaporation, even in cases for which the copolymer composition would suggest a transition to a different equilibrium heterogeneous phase. Recently, Chan et al.[71] demonstrated the formation of PCL-*b*-P4VP spherical micelles with a PCL corona and P4VP core in a 90/10 v/v

solvent mixture of toluene and dichloromethane (DCM). The polymer was first dissolved in DCM, a good solvent for both blocks, and then toluene (a poor solvent for P4VP) was added to induce the formation of ordered structures in solution with a PCL corona.

Here we also used toluene as a preferential solvent for PCL to create ordered structures of a similar polymer, PCL-*b*-P2VP. All of the studies carried out here used a block copolymer with molecular weights of 35.4 kg/mol for the PCL block and 20.9 kg/mol for the P2VP block. AFM images of PCL-*b*-P2VP micelles spin-cast from toluene onto silicon substrates were collected and dynamic light scattering was performed to measure the hydrodynamic diameter. Figure 1A and B show an AFM height and corresponding phase image of PCL-*b*-P2VP micelles cast from toluene. By spin-casting at high speed from dilute (0.01 g/L) solutions, we were able to create films where individual micelles were easily visible with separation distances between adjacent micelles of several hundred nanometers. Line scans through individual micelles (e.g., Figure 1C) were analyzed to determine the distribution of micelle heights and diameters (Table 1). The block copolymer had a PDI of 1.8 and we also observed significant polydispersity in the size of the micelle assemblies. With an average diameter of 103 ± 32 nm and average height of 5.6 ± 2.4 nm, the micelles in the images are spherical structures that have flattened out on the surface upon casting/drying. When imaging spherical particles, AFM image analysis overestimates the particle diameter but provides accurate height data because of tip geometry.[72,73] However, because the micelles are flattened (5.6 nm height vs 103 nm diameter) and have a height of only about one-half of the AFM tip radius, the error in estimated diameter due to tip size is negligible.

Though both PCL and P2VP homopolymers are soluble to at least 10 mg/mL in toluene, based on the prior studies of P2VP block copolymers and the Chan et al. study of PCL-*b*-P4VP, we expected that toluene would preferentially solvate PCL, such that P2VP would form the core of PCL-*b*-P2VP micelles

Table 1. Micelle Size Determination and Analysis by DLS and AFM for As-Assembled Micelles and Ova-TR Loaded Micelles in Toluene[a]

micelle solution	hydrodynamic diameter (D_H; nm)	diameter (dry state AFM; nm ± SD)	height (dry state AFM; nm ± SD)	core diameter (nm)	corona thickness (δ; nm)	$\delta/nl \cos \theta$	$\delta/(\alpha^2 C_\infty nl^2)^{1/2}$
as-assembled	154	103 ± 32	5.6 ± 2.4	28	63	0.24	3.7
ova-TR loaded	157	104 ± 27	5.8 ± 1.7	28	65	0.24	3.8

[a] Number average hydrodynamic radius (D_H) measured by DLS. Diameter and height from AFM image analysis. Core diameter, corona thickness, fully extended chain length ($nl \cos \theta$) and RMS end-to-end distance ($\alpha^2 C_\infty nl^2)^{1/2}$ are calculated as discussed in the Supporting Information.

assembled in toluene. Because the homopolymer solubility data did not clearly suggest the micellar structure, we turned to a micelle-swelling assay to confirm the organization of the micelles. We previously demonstrated the ability to induce rearrangement ("cavitation") of dried substrate-supported polystyrene-*block*-poly(acrylic acid) (PS-*b*-PAA) inverse spherical micelles upon treatment with aqueous solutions.[16] Briefly, when inverse micelles cast and dried on substrates are exposed to a selective solvent for the core polymer block, such as aqueous solutions, the hydrophilic micelle core swells and fractures the glassy PS corona. We subsequently studied this process in more detail[69] and others have reported similar behavior for polystyrene-*block*-poly(2-vinyl pyridine) (PS-*b*-P2VP) micelles.[74,75] We have also observed this rearrangement in PS-*b*-P2VP.[76] In the present case, dried micelle coronas would be composed of a rubbery semicrystalline PCL block ($T_g = -60$ °C, $T_m = 60$ °C). We observed a similar cavitation process for PCL-*b*-P2VP micelles cast onto silicon and exposed to PBS for 16 h. Figure 1D and E are AFM height and phase images showing the polymer rearrangement upon treatment in PBS buffer which selectively swells the P2VP core block. The rearrangement is difficult to observe in the height image due to the relatively small cavity depth compared to the overall micelle height. However, micelle reorganization is clearly observed in the phase image (Figure 1E) and micelle height cross section (Figure 1F). The cavity width and depth is underestimated by the AFM due to the similar dimension of the cavity with the AFM tip. Cavitation of the micelles on exposure to aqueous solutions is consistent with P2VP forming the core of the micelle structures. In addition, similar to work done previously in our own laboratory[9−16] and others,[17−32] we exploited the interaction of vinylpyridine groups with metal salts to successfully load gold salts into the core of the PCL-*b*-P2VP micelles as confirmed by TEM imaging (data not shown). These data collectively support the conclusion that P2VP forms the core of PCL-*b*-P2VP micelles assembled in toluene.

The PCL-*b*-P2VP micelles in toluene had a number average hydrodynamic diameter of 154 nm as determined by DLS (Table 1). This result can be compared to the AFM image data: first, AFM image analysis provides an average particle volume ($V_{micelle}$) by approximating the dried micelles as spherical caps on the substrate

$$V_{micelle} = \pi h(3D^2 + 4h^2)/24 \quad (1)$$

where h and D are the height and diameter of the micelles measured by AFM.

Combining this total dry-state micelle volume with our DLS results, certain molecular-level length scales can then be calculated readily (see Supporting Information for details) to provide internal checks on the micellar size and proposed molecular organization (Table 1). The ratios of the calculated corona thickness (δ) to the fully extended chain length ($nl \cos \theta$) and rms end-to-end distance ($\alpha^2 C_\infty nl^2)^{1/2}$ correlate well with what others have observed for spherical micelles[77−85] and are consistent with the proposed P2VP core/PCL corona micelle structure in toluene.

Characterization of Block Copolymer Self-Assembly in Oleic Acid. For drug delivery applications, we assessed PCL-*b*-P2VP solution behavior in oleic acid, a biocompatible natural fatty acid with very different physical properties compared to toluene. Though oleic acid is comprised of a long nonpolar alkyl chain, the acid endgroup of oleic acid enables hydrogen bonding between oleic acid molecules and between oleic acid and dissolved solutes. Oleic acid is a high viscosity, high boiling point liquid, which precludes AFM imaging of dried substrate-supported micelles, as seen above in toluene, because the solvent evaporation rate is too low. To visualize the polymer assembly in solution we turned to cryogenic transmission electron microscopy (cryoTEM). CryoTEM is a technique that relies upon solvent vitrification to trap molecular and morphological conformations and allow direct imaging of the in situ state of structures in liquids. This technique has been widely applied to aqueous systems, but has found more limited application for continuous oil phases, as recently reviewed.[86] Difficulties in sample preparation include problems in applying a thin film to a TEM grid, particularly for high viscosity solvents, finding a suitable cryogen that is not soluble in the oil phase and imaging vitrified solvents that are often more susceptible to electron beam damage and provide lower contrast compared to aqueous solutions.[86,87]

Here we were able to overcome these difficulties to image PCL-*b*-P2VP in oleic acid. Figure 2A shows a representative cryoTEM image of the spherical structures formed by the copolymer in oleic acid. We analyzed an extensive series of cryoEM images to obtain an average particle size and size distribution presented in Figure 2B, with arrows indicating the average micelle size. The average micelle size was 144 nm with a standard deviation of 59 nm for 262 particles imaged. The particle size is similar to that observed for micelles in toluene and, again, we see significant polydispersity. However, unlike toluene, homopolymer solubility data suggest micelles assemble with a PCL core and a P2VP corona: P2VP homopolymer is soluble in oleic acid at 25 °C, while PCL homopolymer is only soluble above 60 °C and precipitates upon cooling. Both homopolymers tested had a similar M_n to their respective blocks in the copolymer. P2VP hompolymer solubility might be attributed the strong hydrogen bonding character of the nitrogen heteroatom.[88]

Loading of Ovalbumin and Bovine Serum Albumin in Micelles. To determine whether PCL-*b*-P2VP micelles could load proteins into organic phases, we chose ovalbumin (ova; 45 kDa, pI = 4.5) and bovine serum albumin (BSA; 67 kDa, pI = 4.8) as model globular proteins cargos. We quantified protein loading into micelle-containing toluene or oleic acid using fluorescently labeled conjugates of ova (ova-TR) and BSA (BSA-TR) as well as a radiolabeled ova (ova-C[14]) conjugate. Micelles were loaded by mixing 1 mL of 10 g/L micelle solution in toluene or oleic acid with 50 uL of 10 g/L protein solution in PBS. Solutions were centrifuged to separate the aqueous and oil phases after 72 h.

In toluene, loadings of 5.7% wt/wt (weight of protein/weight of P2VP) were achieved for ova and 3.0 wt %/wt for the higher
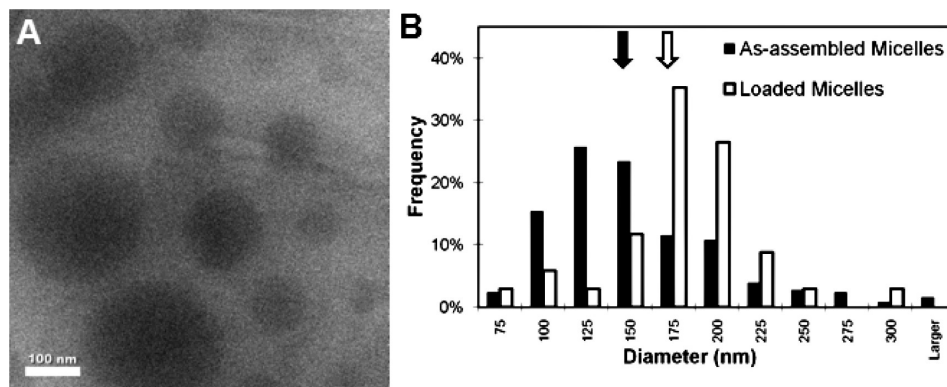
Figure 2. (A) Cryogenic transmission electron microscopy of PCL-*b*-P2VP micelles in oleic acid. (B) Histogram of particle size distribution for as-assembled and ova-TR loaded micelles. Black and white arrows indicate average micelle size for as-assembled and ova-TR loaded micelles, respectively.

Table 2. Loading of Ovalbumin (ova) or Bovine Serum Albumin (BSA) into Polymer Solutions in Toluene or Oleic Acid[a]

solvent	polymer	OVA-TR (%wt/wt; ±SD)	OVA-TR (μg/mL; ±SD)	OVA-C[14] (%wt/wt; ±SD)	OVA-C[14] (μg/mL; ±SD)	BSA-TR (%wt/wt; ±SD)	BSA-TR (μg/mL; ±SD)
oleic acid	PCL-*b*-P2VP	7.8 ± 0.79	290 ± 29	6.5 ± 2.5	241 ± 92.5	1.9 ± 0.68	70 ± 25
oleic acid	PCL	insoluble		n.d.		insoluble	
oleic acid	P2VP	1.9 ± 0.22	190 ± 22	n.d.		0.70 ± 0.041	70 ± 4.1
oleic acid	no polymer		4.8 ± 0.5	0.16 ± 0.19	5.9 ± 7.0	0.039 ± 0.004	3.9 ± 0.4
toluene	PCL-*b*-P2VP	5.7 ± 1.8	211 ± 66.6	n.d.		3.0 ± 0.32	111 ± 12
toluene	PCL	<0.01	<1.0	n.d.		<0.01	<1.0
toluene	P2VP	<0.01	<1.0	n.d.		<0.01	<1.0
toluene	no polymer	<0.01	<1.0	n.d.		<0.01	<1.0

[a] Loading experiments used 10 mg/mL polymer solutions. Protein weight loadings in the polymer solutions are in % wt/(wt of P2VP) for PCL-*b*-P2VP and P2VP homopolymer, and % wt/(wt PCL) for PCL homopolymer. n.d. = not determined.

MW BSA in block copolymer solutions (Table 2). Experiments with P2VP homopolymer, PCL homopolymer, and pure toluene revealed negligible loading of protein into the toluene phase. These results demonstrate the importance of the block copolymer micelle structure for the solubilization of protein for the case of toluene, a highly nonpolar solvent, as the organic phase.

For block copolymer solutions in oleic acid, loadings of 7.8 wt %/wt (weight of protein/weight of P2VP) and 1.9 wt %/wt were achieved for ova and BSA, respectively (Table 2). An ova-TR loading of 7.8 wt %/wt corresponds to transfer of 58% of the ova-TR originally in the aqueous phase into the oleic acid phase by the block copolymer. This degree of protein loading into PCL-*b*-P2VP micelles appeared to be saturating, as experiments using 100 μL of 10 g/L protein solution in PBS did not result in higher amounts of protein being retained in the oil phase. Loading of ovalbumin with fluorescent or radioactive labels showed similar results. As described above, PCL homopolymer is insoluble in oleic acid at room temperature, precipitating upon cooling from 70 °C. Oleic acid from which PCL homopolymer had precipitated and pure oleic acid were unable to solubilize ova or BSA. However, P2VP homopolymer solutions in oleic acid incorporated 1.9% (wt/wt P2VP) ova-TR or 0.70% (wt/wt P2VP) BSA-TR. These results suggest that interactions between oleic acid, P2VP, and the protein support solubilization of ova in the oleic acid phase. Surfactants,[89] including oleic acid[90] and sodium oleate,[91,92] have previously been shown to interact with proteins through a process known as hydrophobic ion pairing[93-95] that can increase protein solubility in an organic phase. This provides a possible mechanism for interaction between ova and oleic acid. But here we observed insignificant loading in pure oleic acid, demonstrating the importance of P2VP.

Because PCL-*b*-P2VP micelles in oleic acid consist of a P2VP corona and PCL core, the observed P2VP homopolymer loading and PCL insolubility suggest that it is the corona of the block copolymer micelles that is sequestering protein in the oleic acid/ block copolymer system. The PCL core is insoluble in both oleic acid and water at room temperature, implying that no significant protein loading can be accommodated. To the best of our knowledge, this is the first demonstration that in continuous oil phases, drug (or protein) cargo loading can occur in the *corona* of block copolymer micelles, as opposed to the more common situation of solute loading in the core of micelles. These results with PCL-*b*-P2VP demonstrate the ability of block copolymers to solubilize protein into either the core or the corona of micelles assembled in organic phases, depending on the balance of interactions between blocks, solvent, and protein.

Characterization of Micelles Loaded with Ovalbumin in Toluene or Oleic Acid. To determine if loading of protein had any effect on the micelle morphology, we characterized the structure of PCL-*b*-P2VP micelles in both toluene and oleic acid after loading of ova-TR. AFM imaging of micelles loaded with ova-TR (Figure 3A) cast from toluene onto silicon showed the same spherical morphology (compare to Figure 1A), and image analysis led to almost identical average dimensions and size distributions (Table 1). In line with the AFM results, DLS experiments gave a hydrodynamic radius of 157 nm for the protein loaded micelles compared to 154 nm for the as-assembled micelles. Each of the characterization techniques indicates that the loading of protein did not have a significant influence on the morphology, size, and size distribution of PCL-*b*-P2VP micelles in toluene. This is consistent with the relatively low weight fraction of protein sequestered within each micelle core.

CryoTEM of ova-loaded micelles in oleic acid showed that the spherical morphology of PCL-*b*-P2VP micelles was unchanged by protein loading, and analysis resulted in a similar
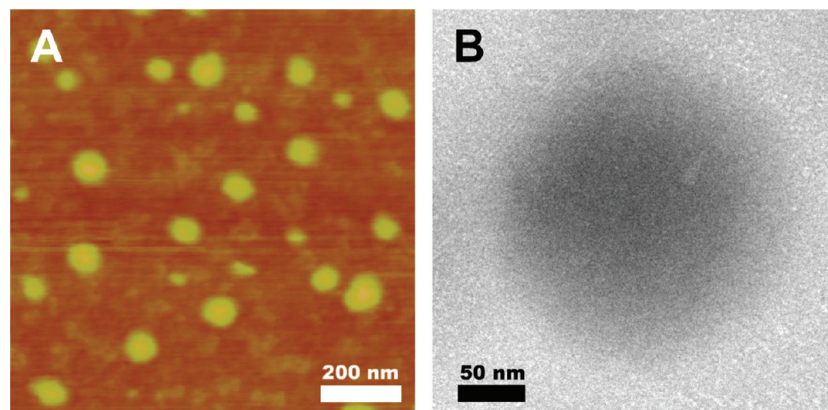
Figure 3. (A) AFM height image of PCL-*b*-P2VP micelles loaded with ova-TR cast from toluene on silicon. Height scale is 20 nm. (B) Cryogenic transmission electron microscopy image of a PCL-*b*-P2VP micelle loaded with ova-TR in oleic acid.
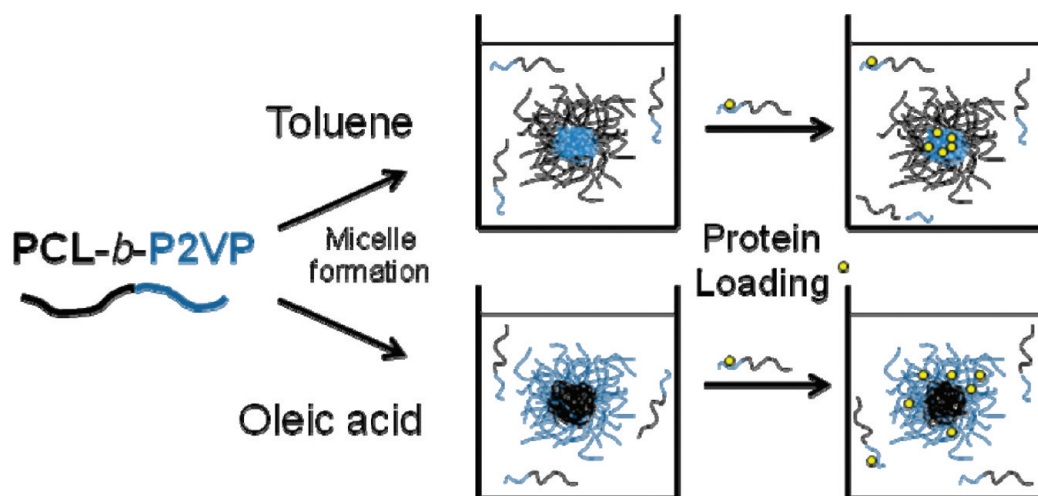

Figure 4. Schematic models for PCl-*b*-P2VP micelle structure and protein loading in toluene and oleic acid.

average size and size distribution (Figure 3B, size histograms overlaid in Figure 2B): The average protein-loaded micelle size is 166 ± 44 for 34 particles imaged. The increase in average micelle size of 22 nm is relatively small compared to the distribution of sizes and may be a result of the small number of loaded micelles that were able to be imaged or may reflect a small increase in micelle dimensions following protein loading.

Summarizing these observations, we propose the following mechanism for micelle loading of protein in our experiments (Figure 4): in solution single block copolymer chains, or unimers, exchange with the micelle assemblies.[70] The P2VP block of the unimer in solution complexes protein, which is then shuttled into a micelle assembly, thereby loading the protein into the micellar structure. This unimer shuttling process sequesters protein molecules into the micelle, regardless of the location of the P2VP block, that is, in the micelle core or corona. When a copolymer molecule leaves the micelle, the protein remains behind, cooperatively associating itself favorably with the P2VP blocks in the micellar structure. The block copolymer is able to load significantly more ova per unit weight of P2VP compared to P2VP homopolymer, showing the importance of the micelle structure for protein loading. For homopolymer solutions, protein would be solubilized by interacting with individual P2VP chains, or groups of P2VP chains that would entropically prefer to be dispersed rather than aggregated. In contrast, protein solubilization would be supported in the micelle

case by the ability of multiple neighboring P2VP chains anchored to the micelle core to cooperatively interact with ova. We hypothesize that the increased potential for cooperative action of multiple P2VP chains in promoting solubilization of each protein molecule is the key to the difference between the homopolymer and block copolymer solutions.

Release of Ovalbumin from PCL-*b*-P2VP Micelles in Oleic Acid. We hypothesized that micelles in biocompatible oils could serve as depots for sustained release of proteins or other drug compounds from oil phases into extracellular fluids in various applications such as topical or oral drug delivery. To investigate the release of protein from micelles we measured the exchange of protein between an oleic acid block copolymer solution loaded with ova-TR and an aqueous reservoir of PBS with 1% BSA. Oleic acid (100 μL) containing 10 g/L PCL-*b*-P2VP loaded with ova-TR (29 ug ova total) was gently layered over 1 mL of an aqueous reservoir (PBS with 1% BSA) in a 1.5 mL microcentrifuge tube, and protein transfer into the aqueous phase during static incubation at 37 °C was recorded over time via fluorescence measurements. Similar to prior studies of small molecule or protein transfer between micelles or nanoparticles in an organic and an aqueous reservoir,[34,36,37] we carried out these experiments under static conditions, to avoid emulsification of the oil phase into droplets in the aq phase, which would be expected to dramatically alter the release kinetics and might not accurately reflect the behavior of, for example, topically applied oil. (However, some mixing of oil with surrounding interstitial fluid would undoubtedly occur
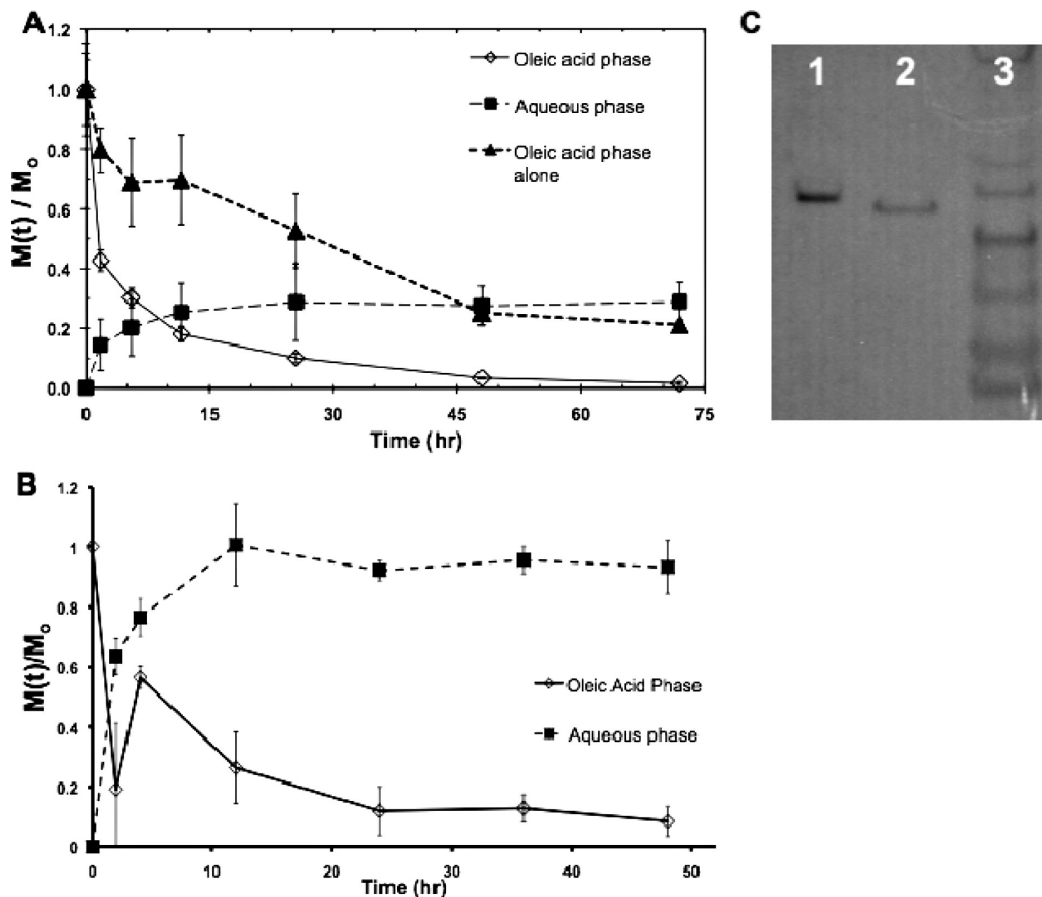
Figure 5. (A) Release of ova-TR from 100 μL of oleic acid/PCL-*b*-P2VP micelle solution layered over 1 mL of a 1% BSA in PBS pH 7.4 reservoir at 37 °C upon static incubation measured by fluorescence. Error bars represent the std dev of four independent fluorescence measurements. "Oleic acid phase" and "aqueous phase" denote protein measurements on the loaded polymer micelle solution and aqueous reservoir solution, respectively. "Oleic acid phase alone" denotes an ova-loaded copolymer micelle solution in oleic acid that was incubated without addition of an aqueous reservoir. $M(t)$ is the mass of ova-TR in the indicated phase at time t, M_0 is the initial mass of ova-TR in the oleic acid phase. (B) Kinetics of ova release from 100 μL of PCL-*b*-P2VP micelles in oleic acid layered over 5 mL of a 1% BSA in PBS aqueous reservoir. (C) SDS PAGE of ova-TR release from oleic acid block copolymer solution into PBS reservoir (no BSA present in reservoir). Lanes: (1) ova-TR released from block copolymer oleic solution; (2) ova-TR stock solution; and (3) protein ladder. The band just above the location of ova-TR in lanes 1 and 2 represents ∼49 kDa standard, and the band just below represents ∼37 kDa standard.
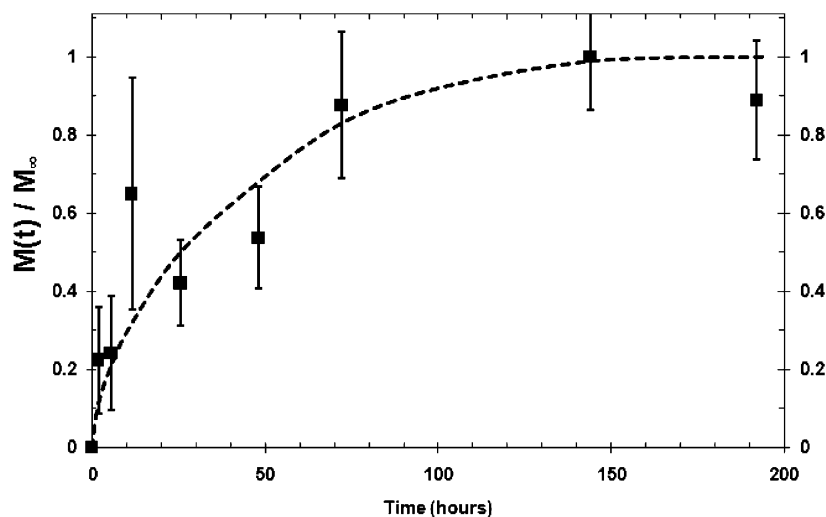

Figure 6. Release of ova-TR from PCL-*b*-P2VP micelles in toluene into an aqueous reservoir of PBS with 1 wt %/v BSA during static incubation in an microcentrifuge tube. Data points represent the amount of ova-TR in the aqueous reservoir and are normalized to the final amount of ova in the aq reservoir (M_∞). Error bars represent standard deviation of three independent experiments. The dotted line is a quide to the eye.

during in vivo applications, which could lead to differences between in vivo release rates and these idealized measurements.)

The release profile of ova-TR from the inverse micelle in oleic acid is shown in Figure 5A.

Release of ova-TR from the micelle phase reached 80% of the maximum released by 12 h and 90% of the maximum by 25 h. The amount of ova-TR in the oleic acid phase dropped to 2% of initial loading by the 72 h time point, however, the amount of ova-TR released into the aqueous phase at the 72 h time point was only 30% of the initial loading (M_0). A series of control experiments was carried out to understand the source of this protein loss. Ova-TR standard solutions in PBS with 1% BSA were completely stable over this time course (data not shown). However, ova-TR-loaded micelles in oleic acid incubated in the absence of an aqueous phase ("oleic acid phase alone", Figure 5A) showed a loss of ova-TR over time, with only 21% of the originally loaded protein remaining at the 72 h time point. Three potential mechanisms for protein loss from the oleic acid phase are (i) protein adsorption to the walls of the centrifuge tube in the oil phase, (ii) slow aggregation of protein in the micelle phase, or (iii) protein aggregation at the oleic acid−water interface. To distinguish between these possibilities, experiments measuring release of ova-TR from different volumes of oleic acid/micelle solutions into fixed volumes of aqueous phase in the same microcentrifuge tubes were performed. In this setup, the oil phase/tube wall interfacial area was steadily increased while the oil/aqueous reservoir interfacial area was held constant. We observed that the amount of ova-TR signal loss scaled linearly with the amount of oleic acid micelle solution volume (data not shown). This suggests that protein lost from the organic phase was either due to adsorption on the tube walls or aggregation within the oil phase, rather than protein aggregation at the oleic acid−water interface. To determine whether the lack of medium exchanges providing rigorous "sink" conditions was responsible for the kinetics of release observed and to gain more insight into the potential mechanisms of protein loss observed, we repeated these release kinetics measurements using a larger aqueous reservoir. The same oil/polymer phase volume of 100 μL was layered over 5 mL of aq phase (50-fold greater than the oleic acid phase volume) in larger 15 mL centrifuge tubes that increased the aqueous phase/oil phase interfacial area by 2.8-fold and decreased the oil phase/tube wall interface by 2.8-fold. Under these conditions, protein release was faster but still sustained over ∼12 h (Figure 5B). Notably, minimal protein loss was observed under these conditions, with protein transfer to the aq. phase plateauing at ∼93% of the quantity originally loaded into the micelle/oil phase. In summary, protein is released more quickly when the oil phase is contacted with a larger aqueous reservoir, but protein loss due to adsorption to the tube walls is suppressed.

We also confirmed the transfer of protein into aqueous phase reservoirs lacking BSA by SDS PAGE analysis (Figure 5C). Importantly, ova-TR release from the block copolymer oil phase showed no signs of aggregation/oligomerization but migrated at a slightly higher molecular weight compared to the ova-TR standard solution, which may reflect some residual association of oleic acid molecules with release protein. The kinetics of ova-TR release from P2VP homopolymer in oleic acid (data not shown) were similar to block copolymer solutions, suggesting a similar release mechanism from PCL-*b*-P2VP and P2VP homopolymer solutions. The key advantage of the block copolymer structure compared to homopolymer P2VP is thus the increased loading of protein into the organic phase achieved per mass of P2VP.

To compare to our oleic acid release data, we measured the release of ova-TR from PCL-*b*-P2VP micelles in toluene. The same experimental setup and geometry as above was used, but due to the volatile nature of toluene, we ran experiments at 25 °C to limit the effect of toluene evaporation on the results (Figure 6). Ova-TR release was complete after ∼100 h, slower than the release kinetics observed for micelles in oleic acid at 37 °C. These release kinetics are similar to what we observed for release of ova-TR from micelles in oleic acid at 25 °C (data not shown).

Conclusions

We characterized the self-assembly of PCL-*b*-P2VP block copolymers in both toluene and a pharmaceutically relevant solvent, oleic acid, and analyzed the loading of two model globular proteins into micelles formed in each of these solvents. In nonpolar toluene, PCL-*b*-P2VP formed spherical micelles (∼150 nm diam.) with a P2VP core and PCL corona, while in oleic acid, the data suggest that micelles (∼150 nm diam.) with a PCL core and P2VP corona were formed. Both ovalbumin and bovine serum albumin could be loaded into micelles in either solvent, demonstrating the ability of PCL-b-P2VP micelles to sequester protein into a P2VP core or P2VP corona in organic phases. Notably, block copolymer micelles formed in oleic acid, where protein was sequestered in the P2VP corona, obtained the highest level of protein loading (∼8 wt %/(wt P2VP)). On contact of these protein-loaded oleic acid/block copolymer solutions with an aqueous reservoir, transfer of protein from the oil phase back into aqueous solution was sustained for 12−30 h. This work illustrates the potential of block copolymer micelles assembled in biocompatible oils to serve as carriers for sustained release of hydrophilic macromolecular cargos.

Supporting Information Available. Detailed explanation and calculation of molecular-level micelle length scales and comparison to literature values. This material is available free of charge via the Internet at http://pubs.acs.org.

References and Notes

(1) Nishiyama, N.; Kataoka, K. *Pharmacol. Ther.* **2006**, *112* (3), 630–648.
(2) Qiu, L. Y.; Zheng, C.; Jin, Y.; Zhu, K. J. E. *Expert Opin. Ther. Pat.* **2007**, *17* (7), 819–830.
(3) Mahmud, A.; Xiong, X. B.; Aliabadi, H. M.; Lavasanifar, A. *J. Drug Targeting* **2007**, *15* (9), 553–584.
(4) Park, J. H.; Lee, S.; Kim, J. H.; Park, K.; Kim, K.; Kwon, I. C. *Prog. Polym. Sci.* **2008**, *33* (1), 113–137.
(5) Peer, D.; Karp, J. M.; Hong, S.; FaroKHzad, O. C.; Margalit, R.; Langer, R. *Nature Nanotechnol.* **2007**, *2* (12), 751–760.
(6) Gaucher, G.; Dufresne, M. H.; Sant, V. P.; Kang, N.; Maysinger, D.; Leroux, J. C. *J. Controlled Release* **2005**, *109* (1−3), 169–188.
(7) Torchilin, V. P. *J. Controlled Release* **2001**, *73* (2−3), 137–172.
(8) Oishi, M.; Sasaki, S.; Nagasaki, Y.; Kataoka, K. *Biomacromolecules* **2003**, *4* (5), 1426–1432.
(9) Bennett, R. D.; Miller, A. C.; Kohen, N. T.; Hammond, P. T.; Irvine, D. J.; Cohen, R. E. *Macromolecules* **2005**, *38* (26), 10728–10735.

(10) Bennett, R. D.; Xiong, G. Y.; Ren, Z. F.; Cohen, R. E. *Chem. Mater.* **2004**, *16* (26), 5589–5595.

(11) Saunders, R. S.; Cohen, R. E.; Schrock, R. R. *Macromolecules* **1991**, *24* (20), 5599–5605.

(12) Bennett, R. D.; Hart, A. J.; Miller, A. C.; Hammond, P. T.; Irvine, D. J.; Cohen, R. E. *Langmuir* **2006**, *22* (20), 8273–8276.

(13) Kane, R. S.; Cohen, R. E.; Silbey, R. *Chem. Mater.* **1996**, *8* (8), 1919–1924.

(14) Sohn, B. H.; Cohen, R. E. *Chem. Mater.* **1997**, *9* (1), 264–269.

(15) Bennett, R. D.; Hart, A. J.; Cohen, R. E. *Adv. Mater.* **2006**, *18* (17), 2274–2279.

(16) Boontongkong, Y.; Cohen, R. E. *Macromolecules* **2002**, *35* (9), 3647–3652.

(17) Terris, B. D.; Thomson, T. *J. Phys. D: Appl. Phys.* **2005**, *38* (12), R199−R222.

(18) Hamley, I. W. *Nanotechnology* **2003**, *14* (10), R39−R54.

(19) Harrison, C.; Park, M.; Chaikin, P. M.; Register, R. A.; Adamson, D. H. *J. Vac. Sci. Technol., B: Microelectron. Nanometer* **1998**, *16* (2), 544–552.

(20) Park, M.; Harrison, C.; Chaikin, P. M.; Register, R. A.; Adamson, D. H. *Science* **1997**, *276* (5317), 1401–1404.

(21) Glass, R.; Arnold, M.; Cavalcanti-Adam, E. A.; Blummel, J.; Haferkemper, C.; Dodd, C.; Spatz, J. P. *New J. Phys.* **2004**, *6*, 101.

(22) Gorzolnik, B.; Mela, P.; Moeller, M. *Nanotechnology* **2006**, *17* (19), 5027–5032.

(23) Jung, J. M.; Kwon, K. Y.; Ha, T. H.; Chung, B. H.; Jung, H. T. *Small* **2006**, *2* (8−9), 1010–1015.

(24) Bratton, D.; Yang, D.; Dai, J. Y.; Ober, C. K. *Polym. Adv. Technol.* **2006**, *17* (2), 94–103.

(25) Haupt, M.; Ladenburger, A.; Sauer, R.; Thonke, K.; Glass, R.; Roos, W.; Spatz, J. P.; Rauscher, H.; Riethmuller, S.; Moller, M. *J. Appl. Phys.* **2003**, *93* (10), 6252–6257.

(26) Fu, Q.; Huang, S. M.; Liu, J. *J. Phys. Chem. B* **2004**, *108* (20), 6124–6129.

(27) Yun, S. H.; Sohn, B. H.; Jung, J. C.; Zin, W. C.; Lee, J. K.; Song, O. *Langmuir* **2005**, *21* (14), 6548–6552.

(28) Yoo, S. I.; Sohn, B. H.; Zin, W. C.; An, S. J.; Yi, G. C. *Chem. Commun.* **2004**, (24), 2850–2851.

(29) Cresce, A. V.; Silverstein, J. S.; Bentley, W. E.; Kofinas, P. *Macromolecules* **2006**, *39* (17), 5826–5829.

(30) Cavalcanti-Adam, E. A.; Bezler, M.; Tomakidi, P.; Spatz, J. P. *J. Bone Miner. Res.* **2004**, *19*, S64−S64.

(31) Cavalcanti-Adam, E. A.; Micoulet, A.; Blummel, J.; Auernheimer, J.; Kessler, H.; Spatz, J. P. *Eur. J. Cell Biol.* **2006**, *85* (3−4), 219–224.

(32) Groll, J.; Albrecht, K.; Gasteier, P.; Riethmueller, S.; Ziener, U.; Moeller, M. *ChemBioChem* **2005**, *6* (10), 1782–1787.

(33) Il Yoo, S.; An, S. J.; Choi, G. H.; Kim, K. S.; Yi, G. C.; Zin, W. C.; Jung, J. C.; Sohn, B. H. *Adv. Mater.* **2007**, *19* (12), 1594+−.

(34) Gross, M.; Maskos, M. *Polymer* **2005**, *46* (10), 3329–3336.

(35) Gao, H.; Jones, M. C.; Tewari, P.; Ranger, M.; Leroux, J. C. *J. Polym. Sci., Part A: Polym. Chem.* **2007**, *45* (12), 2425–2435.

(36) Gao, H.; Jones, M. C.; Chen, J.; Prud'homme, R. E.; Leroux, J. C. *Chem. Mater.* **2008**, *20* (9), 3063–3067.

(37) Jungmann, N.; Schmidt, M.; Ebenhoch, J.; Weis, J.; Maskos, M. *Angew. Chem., Int. Ed.* **2003**, *42* (15), 1714–1717.

(38) Ballou, W. R.; Reed, J. L.; Noble, W.; Young, N. S.; Koenig, S. *J. Infect. Dis.* **2003**, *187* (4), 675–678.

(39) O'Hagan, D. T.; Wack, A.; Podda, A. *Clin. Pharmacol. Ther.* **2007**, *82* (6), 740–744.

(40) Thong, H. Y.; Zhai, H.; Maibach, H. I. *Skin Pharmacol. Physiol.* **2007**, *20* (6), 272–282.

(41) Williams, A. C.; Barry, B. W. *Adv. Drug Delivery Rev.* **2004**, *56* (5), 603–618.

(42) Sinha, V. R.; Kaur, M. P. *Drug Dev. Ind. Pharm.* **2000**, *26* (11), 1131–1140.

(43) Aungst, B. J. *J. Pharm. Sci.* **2000**, *89* (4), 429–442.

(44) Rizvi, S.; Camci, C.; Yong, Y.; Parker, G.; Shrago, S.; Stokes, K.; Wright, H.; Sebastian, A.; Gurakar, A. *Transplant. Proc.* **2006**, *38* (9), 2993–2995.

(45) Dawson, L. A.; Guha, C. *Cancer J.* **2008**, *14* (2), 111–116.

(46) Johnson, N. P.; Kwok, R.; Stewart, A. W.; Saththianathan, M.; Hadden, W. E.; Chamley, L. W. *Hum. Reprod.* **2007**, *22* (11), 2857–2862.

(47) Hagen, A. J.; Hatton, T. A.; Wang, D. I. C. *Biotechnol. Bioeng.* **2006**, *95* (2), 285–294.

(48) Liu, Y.; Dong, X. Y.; Sun, Y. *Sep. Purif. Technol.* **2007**, *53* (3), 289–295.

(49) Liu, Y.; Dong, X. Y.; Sun, Y. *J. Colloid Interface Sci.* **2006**, *297* (2), 805–812.

(50) Liu, Y.; Dong, X. Y.; Sun, Y. *Biochem. Eng. J.* **2006**, *28* (3), 281–288.

(51) Liu, Y.; Dong, X. Y.; Sun, Y. *J. Colloid Interface Sci.* **2005**, *290* (1), 259–266.

(52) Hebbar, H. U.; Sumana, B.; Raghavarao, K. S. M. S. *Bioresour. Technol.* **2008**, *99* (11), 4896–4902.

(53) Hebbar, H. U.; Raghavarao, K. S. M. S. *Process Biochem. (Amsterdam, Neth.)* **2007**, *42* (12), 1602–1608.

(54) Goto, M.; Ono, T.; Nakashio, F.; Hatton, T. A. *Biotechnol. Bioeng.* **1997**, *54* (1), 26–32.

(55) Sugiura, S.; Ichikawa, S.; Sano, Y.; Nakajima, M.; Liu, X. Q.; Seki, M.; Furusaki, S. *J. Colloid Interface Sci.* **2001**, *240* (2), 566–572.

(56) Ichikawa, S.; Sugiura, S.; Nakajima, M.; Sano, Y.; Seki, M.; Furusaki, S. *Biochem. Eng. J.* **2000**, *6* (3), 193–199.

(57) New, R. R. C.; Kirby, C. J. *Adv. Drug Delivery Rev.* **1997**, *25* (1), 59–69.

(58) Jones, M. C.; Tewari, P.; Blei, C.; Hales, K.; Pochan, D. J.; Leroux, J. C. *J. Am. Chem. Soc.* **2006**, *128* (45), 14599–14605.

(59) Porter, C. J. H.; Charman, W. N. *Adv. Drug Delivery Rev.* **1997**, *25* (1), 71–89.

(60) Holm, R.; Mullertz, A.; Pedersen, G. P.; Kristensen, H. G. *Pharm. Res.* **2001**, *18* (9), 1299–1304.

(61) Wasan, K. M. *Drug Dev. Ind. Pharm.* **2002**, *28* (9), 1047–1058.

(62) Strickley, R. G. *Pharm. Res.* **2004**, *21* (2), 201–230.

(63) Fukui, H.; Murakami, M.; Yoshikawa, H.; Takada, K.; Muranishi, S. *J. Pharmacobio. Dyn.* **1987**, *10* (6), 236–242.

(64) Tsutsumi, K.; Obata, Y.; Takayama, K.; Loftsson, T.; Nagai, T. *Drug Dev. Ind. Pharm.* **1998**, *24* (8), 757–762.

(65) Aungst, B. J. *Pharm. Res.* **1989**, *6* (3), 244–247.

(66) Gupta, R. K.; Varanelli, C. L.; Griffin, P.; Wallah, D. F. H.; Siber, G. R. *Vaccine* **1996**, *14* (8), R1−R1.

(67) Qu, S.; Zhang, X. W.; Gao, Y.; You, J. B.; Fan, Y. M.; Yin, Z. G.; Chen, N. F. *Nanotechnology* **2008**, (13), 19. − .

(68) Mossmer, S.; Spatz, J. P.; Moller, M.; Aberle, T.; Schmidt, J.; Burchard, W. *Macromolecules* **2000**, *33* (13), 4791–4798.

(69) Miller, A. C.; Bennett, R. D.; Hammond, P. T.; Irvine, D. J.; Cohen, R. E. *Macromolecules* **2008**, *41* (5), 1739–1744.

(70) Moffitt, M.; Khougaz, K.; Eisenberg, A. *Acc. Chem. Res.* **1996**, *29* (2), 95–102.

(71) Chan, S. C.; Kuo, S. W.; Lu, C. H.; Lee, H. F.; Chang, F. C. *Polymer* **2007**, *48* (17), 5059–5068.

(72) Yang, D. Q.; Xiong, Y. Q.; Guo, Y.; Da, D. A.; Lu, W. G. *J. Mater. Sci.* **2001**, *36* (1), 263–267.

(73) Legleiter, J.; DeMattos, R. B.; Holtzman, D. M.; Kowalewski, T. *J. Colloid Interface Sci.* **2004**, *278* (1), 96–106.

(74) Cong, Y.; Zhang, Z. X.; Fu, J.; Li, J.; Han, Y. C. *Polymer* **2005**, *46* (14), 5377–5384.

(75) Li, X.; Tian, S. J.; Ping, Y.; Kim, D. H.; Knoll, W. *Langmuir* **2005**, *21* (21), 9393–9397.

(76) Miller, A. C. Amphiphilic Block Copolymer Micelles: Creation of Functional Nanocavities and Their use as Nanocontainers for Controlled Release. PhD Thesis, Massachusetts Institute of Technology, Cambridge, 2008.

(77) Colombani, O.; Ruppel, M.; Burkhardt, M.; Drechsler, M.; Schumacher, M.; Gradzielski, M.; Schweins, R.; Muller, A. H. E. *Macromolecules* **2007**, *40* (12), 4351–4362.

(78) Cogan, K. A.; Gast, A. P.; Capel, M. *Macromolecules* **1991**, *24* (24), 6512–6520.

(79) Mcconnell, G. A.; Gast, A. P.; Huang, J. S.; Smith, S. D. *Phys. Rev. Lett.* **1993**, *71* (13), 2102–2105.

(80) Moffitt, M.; Yu, Y. S.; Nguyen, D.; Graziano, V.; Schneider, D. K.; Eisenberg, A. *Macromolecules* **1998**, *31* (7), 2190–2197.

(81) Schillen, K.; Yekta, A.; Ni, S. R.; Farinha, J. P. S.; Winnik, M. A. *J. Phys. Chem. B* **1999**, *103* (43), 9090–9103.

(82) Zhang, L. F.; Barlow, R. J.; Eisenberg, A. *Macromolecules* **1995**, *28* (18), 6055–6066.

(83) Brown, D. S.; Dawkins, J. V.; Farnell, A. S.; Taylor, G. *Eur. Polym. J.* **1987**, *23* (6), 463–467.

(84) Mcconnell, G. A.; Lin, E. K.; Gast, A. P.; Huang, J. S.; Lin, M. Y.; Smith, S. D. *Faraday Discuss.* **1994**, (98), 121–138.

(85) Park, S. Y.; Chang, Y. J.; Farmer, B. L. *Langmuir* **2006**, *22* (26), 11369–11375.

(86) Cui, H.; Hodgdon, T. K.; Kaler, E. W.; Abezgauz, L.; Danino, D.; Lubovsky, M.; Talmon, Y.; Pochan, D. J. *Soft Matter* **2007**, *3* (8), 945–955.

(87) Danino, D.; Gupta, R.; Satyavolu, J.; Talmon, Y. *J. Colloid Interface Sci.* **2002**, *249* (1), 180–186.

(88) Hameed, N.; Guo, Q. P. *Polymer* **2008**, *49* (4), 922–933.

(89) Paradkar, V. M.; Dordick, J. S. *Biotechnol. Bioeng.* **1994**, *43* (6), 529–540.

(90) Hamilton, J. A.; Cistola, D. P. *Proc. Natl. Acad. Sci. U.S.A.* **1986**, *83* (1), 82–86.

(91) Li, Y.; Jiang, H. L.; Zhu, K. J. *J. Mater. Sci.: Mater. Med.* **2008**, *19* (2), 827–832.

(92) Yoo, H. S.; Choi, H. K.; Park, T. G. *J. Pharm. Sci.* **2001**, *90* (2), 194–201.

(93) Dai, W. G.; Dong, L. C. *Int. J. Pharm.* **2007**, *336* (1), 58–66.

(94) Powers, M. E.; Matsuura, J.; Brassell, J.; Manning, M. C.; Shefter, E. *Biopolymers* **1993**, *33* (6), 927–932.

(95) Meyer, J. D.; Manning, M. C. *Pharm. Res.* **1998**, *15* (2), 188–193.